ELSEVIER

Journal of Luminescence 64 (1995) 173–179

JOURNAL OF LUMINESCENCE

High-temperature spectral hole burning on Sm-doped single crystal materials of PbFCl family

R. Jaaniso*, H. Bill

Department of Physical Chemistry, University of Geneva, 30 quai Ernest-Ansermet, CH-1211 Geneva 4, Switzerland

Received 21 September 1994; revised 25 November 1994; accepted 17 December 1994

Abstract

Basic properties relevant to spectral hole burning (homogeneous and inhomogeneous spectral broadening, hole burning and filling mechanisms) are investigated in $Me^{I}_{y}Me^{II}_{1-y}FX^{I}_{x}X^{II}_{1-x}:Sm^{2+}$ (Me = Ca,Sr,Ba; X = Cl,Br,I) single crystals. The relations between the spectral characteristics of $^5D_{0,1}-^7F_0$ transitions and the material structure are described. Hole stability is investigated up to 430 K and is shown to be determined by ionic diffusion.

1. Introduction

Realization of the room-temperature hole burning on Sm-doped mixed crystals [1,2] and glasses [3–5] is an exciting milestone if to consider the existence of potential applications of the spectral hole burning method [6]. It includes also the possibilities towards new insights into the disordered materials and we have therefore extended the studies, first performed on $SrFCl_{0.5}Br_{0.5}:Sm^{2+}$, to a wider class of single crystal materials with general composition $Me^{I}_{y}Me^{II}_{1-y}FX^{I}_{x}X^{II}_{1-x}:Sm^{2+}$ (Me = Ca, Sr,Ba; X = Cl,Br,I).

The persistence of the basic PbFCl-type structure (P4/nmm space group) for different series of these mixed crystals [7,8] provides a possibility to study the hole burning characteristics in dependence of the material composition. One can introduce the closest possible ionic substitutions (Ca → Sr → Ba; Cl → Br → I), or follow even smaller (and gradual) changes by varying y and x. The latter possibility, together with the relative ease to model the substitutional disorder, allowed to describe the inhomogeneous broadening in a very detailed manner on the example of $SrFCl_xBr_{1-x}:Sm^{2+}$ [9]. The first part of the present paper deals with spectral broadening parameters (in particular, their dependence from host structure and composition are described). The above mentioned reasons make it also enticing to study the electronic and ionic movements through the hole burning at elevated temperatures. Corresponding results are given in the second part of the paper.

*Corresponding author. Permanent address: Institute of Physics, Estonian Academy of Sciences, Tartu, Estonia.

2. Results. 1. Spectral characteristics

The scheme of Sm^{2+} energy levels in the title compound family is shown in Fig. 1. The spectra of the two lower-frequency 4f–4f transitions

0022-2313/95/$09.50 © 1995 – Elsevier Science B.V. All rights reserved
SSDI 0022-2313(95)00038-0

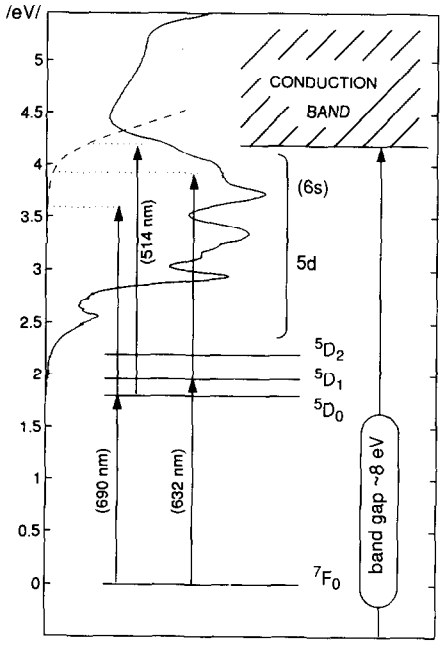

Fig. 1. Energy level scheme of Sm^{2+} in PbFCl family compounds. The location of the (5d,6s) levels are illustrated by the room-temperature absorption spectrum of $SrFCl_{0.5}Br_{0.5}:Sm^{2+}$.

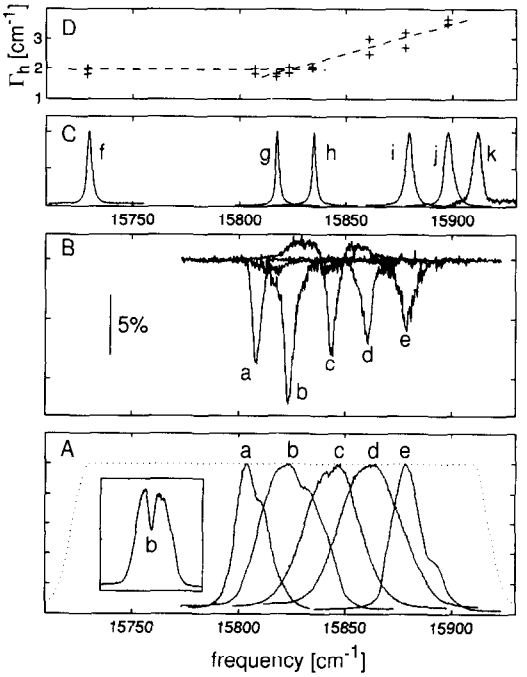

Fig. 2. Room-temperature spectral data for $^5D_1$–$^7F_0$ transition. Excitation spectra (A,C) and spectral holes (B) in $Ca_{0.2}Sr_{0.8}FCl$ (a), $SrFCl_{0.5}Br_{0.5}$ (b), $Sr_{0.8}Ba_{0.2}FCl_{0.2}Br_{0.8}$ (c), $Sr_{0.5}Ba_{0.5}FCl_{0.5}Br_{0.5}$ (d), $BaFCl_{0.5}Br_{0.5}$ (e), CaFCl (f), SrFCl (g), SrFBr (h), BaFCl (i), BaFBr (j), and BaFI (k). Inset in (A) shows ~ 40% hole in spectrum (b). (D) homogeneous line width Γ_h, shown for different compounds as the function of transition frequency.

($^5D_{0,1}$–$^7F_0$) were observed in all the materials, virtually without any background from the higher-energy parity-allowed 4f–5d transitions. In Figs. 2(A) and (B), the excitation spectra and the spectral holes burnt at room temperature are shown for a set of crystals which cover the spectral region of about 100 cm^{-1} for $^5D_1$–$^7F_0$ transition.

The spectra were recorded by using a tunable dye laser (CR699-21 without intracavity etalons; the birefringent filter was turned with stepper motor) and by detecting the fluorescence through a low-pass color filter with a photomultiplier tube (R2949) or a Si-photodiode (S1226-44BQ). The crystals were grown by the Czochralski method as described previously [1, 8]. The dimensions of the crystal platelets used in the hole burning experiments were typically $5 \times 5 \times 0.2$ mm.

The *inhomogeneous broadening* of the mixed crystal spectra is basically determined by a small cluster, consisting of about 5–10 closest neighbors to Sm^{2+} [9, 10]. For example, a single $Cl^- \leftrightarrow Br^-$ substitution in the first coordination sphere produces an average change in the $^5D_{0,1}$–$^7F_0$ transition frequency of about 8 cm^{-1}. The spectral distribution of the possible clusters with 1 axial and 4 nonaxial X^--type ligands (Fig. 3) gives the main contribution to the total line width ($\Gamma_{ih} \approx 33$ cm^{-1}) in $SrFCl_{0.5}Br_{0.5}$. The role of the 5 next nearest sites is shown to be also relatively significant (substitutional shifts ranging from 1 to 5 cm^{-1}). The outer part of the crystal produces smoothing of the discrete structure but adds only about 5% to the variance of the overall inhomogeneous spectral distribution. The outer crystal surrounding has, however, a larger impact on the relative displacements of the spectra: parallel shifts of the local cluster frequencies by 40–80 cm^{-1} are observed if x or y changes from 1 to 0.

According to the crystallochemical studies [7, 8], the parent compounds with 'neighbor' ions (Cl–Br, Br–I, Sr–Ba, Ca–Sr) can be mixed in arbitrary ratios, whereas for bigger mismatch (Cl–I, Ca–Ba) the

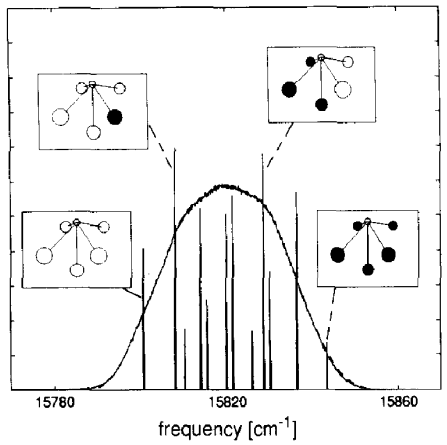

Fig. 3. Inhomogeneous fluorescence spectrum of $^5D_1$–$^7F_0$ transition (T = 30 K) in $SrFCl_{0.5}Br_{0.5}$ and spectral distribution of ligand clusters according to Ref. [9]. The four examples from 12 different cluster configurations are shown. The Cl^- and Br^- ligands around central Sm^{2+} are depicted by filled and empty circles, respectively.

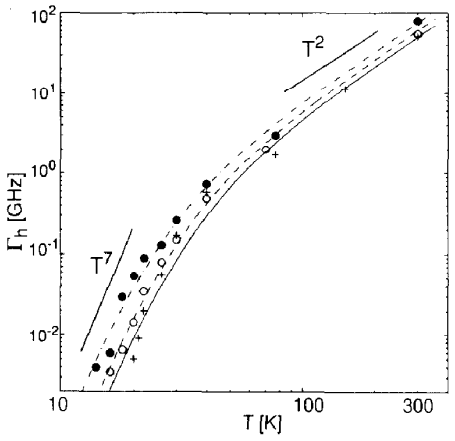

Fig. 4. Temperature dependence of the $^5D_1(E)$–$^7F_0(A_1)$ transition homogeneous line width Γ_h in SrFCl (+), $SrFCl_{0.5}Br_{0.5}$ (○), and $Sr_{0.5}Ba_{0.5}FCl_{0.5}Br_{0.5}$ (●) crystals. The results of the fit with formula (1) are shown with solid, dashed, and chain line, respectively.

solubility is limited to about 10%. These observations agree with the empirical Hume–Rothery's rule for the binary solid solutions [11] which states that if the difference between the lattice parameters of the parent compounds is bigger than about 15%, then the solubility is severely limited. This fact limits the possibilities to enlarge the frequency variations of the local cluster by introducing bigger substitutional changes in ionicity and in ionic volume. Another factor limiting the value of Γ_{ih} can be demonstrated by comparing spectra (b) and (d) in Fig. 2(A). There is practically no additional broadening in $Sr_{0.5}Ba_{0.5}FCl_{0.5}Br_{0.5}$ as compared to $SrFCl_{0.5}Br_{0.5}$. Thus, the substitutions become partially correlated in case of double mixing.

In order to clarify the mechanism of *homogeneous line broadening*, the temperature dependence of the homogeneous line width Γ_h was investigated. Previous studies on certain members of the title compound family revealed the characteristic $\Gamma_h \sim T^2$ dependence above 100 K (dephasing by second order coupling to Debye phonons) [2, 12], but at low temperatures (T 20 K) an anomalous ('glass-like') $\Gamma_h \sim T^{1.3}$ dependence was found in the powder samples of some mixed compounds [2].

We used the following approaches to collect the data for $^5D_1(E)$–$^7F_0(A_1)$ transition in different temperature regions: i) hole burning by pumping the ground state nuclear quadrupolar sublevels (NQS) of Sm^{2+} [13] (10–22 K); ii) two-photon (gated) hole burning [14] (22–40 K in ordered crystals; 22–300 K in mixed crystals); iii) measurement of the fluorescence lines (70–300 K in ordered crystals). In order to minimize the effect of saturation broadening at hole burning [6], shallow holes with relative depths below 1.5% were probed (at fully saturated hole depths of 20%). In case of fluorescence measurements (iii) the true homogeneous part was extracted by deconvolution with a respective low-temperature spectrum (T = 30 K).

The Fig. 4 illustrates the results for three compounds with different degrees of disorder. In all cases the data could be fitted over the whole temperature range with formula [15]

$$\Gamma_h(T) = \bar{\alpha}(T/T_D)^7 \int_0^{T_D/T} \frac{dx x^6 e^x}{(e^x - 1)^2}, \qquad (1)$$

which describes the Raman-type dephasing in the Debye approximation. Here T_D is the Debye temperature and $\bar{\alpha}$ is the coupling strength. In comparison with Refs. [2, 12], both parameters could be obtained from the fit (see Table 1) and there is a clear turnover to the $\Gamma_h \sim T^7$ law at lower

Table 1
Coupling parameters $\bar{\alpha}$ for Sm^{2+} $^5D_1(E)$–$^7F_0(A_1)$ transition and effective Debye temperatures T_D

Host crystal	$\bar{\alpha}$ [GHz]	T_D [K]
SrFCl	103	190
$SrFCl_{0.5}Br_{0.5}$	103	173
$Sr_{0.5}Ba_{0.5}FCl_{0.5}Br_{0.5}$	87	143

temperatures. In addition, a clear dependence of the broadening parameters on the crystal composition can be seen. The effective Debye temperatures T_D obtained from the fit are well correlated with the values of the Raman frequencies (see Ref. [16] and references therein) or with the calculated T_D values [17], but are smaller than the latter ones or the values measured by other techniques. A reasonable comparison is possible for BaFCl [18] and this gives the scaling factor of 1.8 times. The material dependence of the homogeneous line width at room temperature is illustrated in Fig. 2(D).

We note that by using gated hole burning below 20 K wider hole widths were observed and the temperature law (half hole width $\sim T^{1\div 2}$) was close to that observed in Ref. [2]. As the excitation intensities at gated hole burning were significantly higher than those used in NQS pumping (of the order of 10 and 0.01 mW/cm^2, respectively), we concluded that gated hole burning leads to power-broadened holes at low temperatures and hence does not yield the proper values for Γ_h. At the highest temperature for stable NQS pumping (22 K) the hole burning with two different mechanisms (i and ii) gave the same values of Γ_h within $\pm$ 10%.

II. Hole burning mechanism and thermal stability

In the first hole burning study on the present type of materials ($BaFCl:Sm^{2+}$) [14] the gated two-photon hole burning was ascribed to the photoionization of Sm^{2+}. The two following processes were proposed ($Z^{(0)}$ stands for an electron trap of unknown origin, indexes A and B denote different lattice sites):

$$nSm^{2+} + mZ^{(0)} \rightarrow (n-k)Sm^{2+} + kSm^{3+} + kZ^{(-)} + (m-k)Z^{(0)},$$

$$Sm_A^{2+} + Sm_B^{3+} \leftrightarrow Sm_A^{3+} + Sm_B^{2+}.$$

In the pre-irradiated samples (λ_{irr} = 458–514 nm) of $SrFCl_{0.5}Br_{0.5}:Sm^{2+}$ the observed two-photon character together with the redistribution of the intensity (see e.g. the hole 'c' in Fig. 2(B)) was found to be consistent with process (II) [1]. The increased signal outside the hole was explained to originate from the initially trivalent samarium ions which were converted during hole burning into Sm^{2+} with statistically distributed resonant frequencies. In Sm-doped ionic glasses the room-temperature spectral hole burning has been attributed to process (I) [3–5].

We derived the following equation for the time evolution of the Sm^{2+} spectral distribution $\rho(\nu,\tau)$ in the presence of both processes:

$$\frac{d\rho(\nu,\tau)}{d\tau} = -\rho(\nu,\tau)\Lambda(\nu-\nu_b) + \frac{C\rho_o(\nu)-\rho(\nu,\tau)}{\sigma+(1-\sigma)[C-\int d\nu'\rho(\nu',\tau)]} \int d\nu'\rho(\nu',\tau)\Lambda(\nu'-\nu_b), \quad (2)$$

where $\Lambda(\nu-\nu_b) = (\Gamma_h/2)^2/[(\Gamma_h/2)^2+(\nu-\nu_b)^2]$, $\rho_o(\nu)$ is the total spectral distribution of Sm in bivalent state, σ is the ratio of electron trapping cross-sections of $Z^{(0)}$ and Sm^{3+}, respectively, and $C = [Sm^{2+}+Sm^{3+}]/[Z^{(0)}+Sm^{3+}]$ is the ratio of the Sm concentration to the concentration of the electron traps. The parameter τ is proportional to the time (t) and to the peak cross-section of the homogeneous absorption line (κ). For a two-photon process $\tau = tI_b^2\kappa\eta_{eff}$, where I_b is the photon flux during hole burning and the last factor depends on the excited state absorption cross-section, on the intercenter relaxation rates, and on the electron escape yield. The quantity $\rho(\nu,\tau)$ is defined as the number of Sm^{2+} ions with resonant frequencies in the interval $\nu \div \nu + d\nu$

relative to the total number of electron traps. It is normalized as follows:

$$\int_0^\infty d\nu \rho(\nu,\tau) = [Sm^{2+}]/[Z^{(0)} + Sm^{3+}]. \quad (3)$$

On deriving Eq. (2) the electron trapping probability at $Z^{(0)}$, or at Sm^{3+}, respectively, was assumed to be proportional to the concentration and trapping cross-section of the corresponding species. The Eqs. (I) and (II) imply that both the total number of Sm ions ($Sm^{2+} + Sm^{3+}$) and the total number of electron traps ($Z^{(0)} + Sm^{3+}$) remain constant in time. There are four different species involved in (I) and (II) but because of these 'conservation laws' the hole burning kinetics depends only on two relative concentrations: on C and on initial parameter $C_0^{(2+)} = [Sm^{2+}]/[Z^{(0)} + Sm^{3+}]|_{\tau=0}$.

The spectral changes are well described with the given equation. In all crystals we initially never see the presence of Sm^{3+} (holes a,b,d,e in Fig. 2(B)), but after pre-irradiation the second process (II) is dominant. The parameter C was found to be strongly sample dependent – the value of C^{-1} varied from less than 1% up to values of the order of one. In the latter cases hole depths of 40% could be easily achieved (Fig. 2(A) inset). The parameter σ could be estimated by modelling the situation when the hole burning at ν_2 fills up the hole burnt before at $\nu_1 \neq \nu_2$. The trapping cross-section was estimated to be at least one order larger for Sm^{3+} than for $Z^{(0)}$. We will describe below one example of modelling by Eq. (2) (multiple hole burning in Fig. 5), whereas a more detailed analysis of hole burning kinetics will be given elsewhere [19].

The burning of two or more holes into the spectrum is always accompanied by some filling of the holes burnt at earlier times. The filling effect may thought to be reduced if the holes at different frequencies are burnt simultaneously. The following procedure was used for (quasi-)simultaneous multiple hole burning. At first, short exposures during time interval Δt were made at different frequencies, one after the other. Then this procedure was repeated N times so that the total exposure time $N\Delta t$ was equal to the characteristic time found from the experiments with a single hole. The result obtained

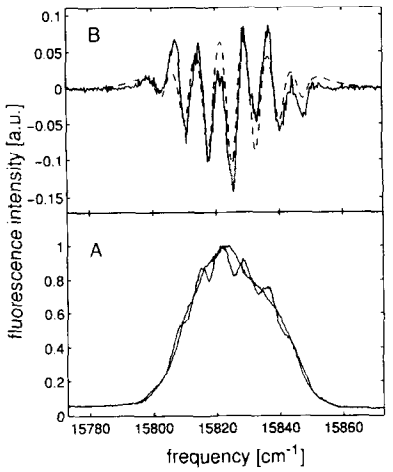

Fig. 5. (A) Excitation spectra of $SrFCl_{0.5}Br_{0.5}:Sm^{2+}$ before and after quasi-simultaneous multiple hole burning ($\Delta t = 3$ s, $N = 20$, spectral interval 7.5 cm^{-1}, burning power 100 mW, spot diameter $\approx$ 0.2 mm). (B) Experimental (solid line) and computer simulated (dashed line) difference signals; $T = 296$ K.

by burning 7 holes with a 7.5 cm^{-1} spectral interval is shown on Fig. 5. As can be seen, all the holes are present and the signal is increased only between the holes. In order to compare the result with the solution of Eq. (2), $\Lambda(\nu - \nu_b)$ was replaced by a sum over all burn frequencies ν_{bi} ($i = 1,...,7$): $\Sigma\Lambda(\nu - \nu_{bi})$. The following parameters were used in this numerical simulation: $C = 1.5$, $\sigma = 0.1$, $\Gamma_h = 2$ cm^{-1}, $\Gamma_{ih} = 28$ cm^{-1} (the inhomogeneous distribution $\rho_0(\nu)$ was approximated by a Gaussian curve). The sample used in the experiment was pre-irradiated at λ_{irr} for a relatively long time (1 h). It was therefore assumed that the irreversible process (I) had been completed before the hole burning and the concentration of $Z^{(0)}$ traps was set to zero. In this case only one concentration parameter had to be adjusted as $C_0^{(2+)} = C - 1$.

Gated hole burning at $T = 296$ K was realized on the $^5D_0$–$^7F_0$ transition (Fig. 6). The Ar^+ laser line at 514.5 nm was used for the second excitation step, similarly as in Ref. [14] for $BaFCl:Sm^{2+}$ at 2 K. At low-temperatures the f–f absorption peak cross-section κ exceeds the f–d absorption cross-section by several orders, whereas at room temperature the corresponding values are practically equal for $\lambda_g = 514$ nm. As a consequence, the gating effect is accompanied by non-selective excitation

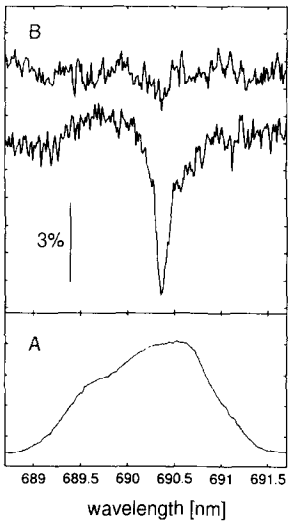

Fig. 6. $^5D_0$–$^7F_0$ transition spectrum (A) and difference signals (B) for single-color (upper curve; $\lambda_b = 690.4$ nm, 20 mW) and gated (lower curve; $\lambda_b = 690.4$ nm, 20 mW; $\lambda_g = 514.5$ nm, 1 mW) hole burning in $SrFCl_{0.5}Br_{0.5}$; $T = 296$ K.

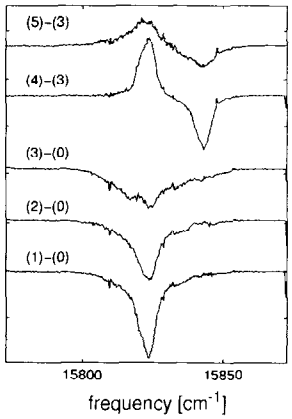

Fig. 7. Hole burning and filling in $SrFCl_{0.5}Br_{0.5}:Sm^{2+}$ at 325 K. The differences of two spectra are shown. The spectra were measured in a following sequence: (0) initial spectrum; (1) 1 min after hole burning at $\nu_1 = 15823$ cm^{-1}; (2) 20 min after hole burning; (3) 120 min after hole burning; (4) 1 min after second hole burning at $\nu_2 = 15843$ cm^{-1}; (5) 60 min after second hole burning.

(and burning) through the f–d absorption. To avoid this effect, relatively low intensities of the green light are required. The effective gating at as small ratio of the gating to resonant light intensities as 1:20 indicates that the 2-quantum energies lie on the exponential tail of the ionization efficiency (see Fig. 1). For the $^5D_1$–$^7F_0$ transition the energy of two resonant quanta is sufficient for self-gating at room temperature.

The evolution of the holes after burning was also investigated at and above room temperature. In both $SrFCl_{0.5}Br_{0.5}$ and $BaFCl_{0.5}Br_{0.5}$ hosts hole decay was observed at 297 K. For the hole depth (which decreased in time approximately exponentially) the following decay times were determined: 24 h for Sr-compound and 5 min for Ba-compound. The decay times measured between 297 and 350 K followed the Arrhenius law with the activation energies of 1.16 eV in $SrFCl_{0.5}Br_{0.5}$ and 1.05 eV in $BaFCl_{0.5}Br_{0.5}$, and with a pre-exponential factor $A = (8 \pm 4) \times 10^{14}$ s^{-1}.

The presence of spectral diffusion (see hole broadening in Fig. 7) indicates that ionic movement is involved in the underlying process. The appearance of a sharp antihole in the spectrum ((4)-(3)) in Fig. 7 illustrates further that Sm^{3+} ions (produced by the first hole burning in this experiment) acted as the electron traps at the second hole burning i.e. Sm^{3+} remained unaffected in the time scale of spectral diffusion (some hours in case of Fig. 7). Consequently, thermally activated reverse reactions to (I) or to (II) [20] do not occur in this time scale. Furthermore, the initially ionized Sm^{2+} ions returned, after the cycle $Sm^{2+} \rightarrow Sm^{3+} \rightarrow Sm^{2+}$, to their original frequencies (the antihole is as sharp as the original hole). One can conclude that the ionic diffusion was absent in the vicinity of uncompensated Sm^{3+}. In other words, Sm^{3+} freezes its environment. This happens in a quite significant manner as the antihole was observed even after cycling the crystals up to 400 K before the second hole burning.

The value of the pre-exponential factor can be expected to be about 4×10^{13} s^{-1} for a single jumping ion. The factor 4 arises from the coordination number and the frequency factor 10^{13} s^{-1} is actually the upper limit one can obtain by using the values of Cl/Br–Sr stretching mode vibrations (135–300 cm^{-1}) [16] or the scaled values of the Debye frequency (≈ 200 cm^{-1}). Comparison with the above given experimental value of A indicates that the spectral diffusion should result at least from 10 independent movements. The latter

number coincides approximately with the number of sites around Sm^{2+} impurity in which the Cl–Br substitutions are able to produce spectral shifts bigger than half a hole width (see Section I). Hence, the hole broadening may be explained as a result of X-type halogen self-diffusion, which results in the redistribution of Cl and Br ions in Sm^{2+} environment. The most probable mechanism is a ring-type direct interchange (see, e.g. Ref. [21]) of three or four neighboring Cl and Br ions. The activation energy is shown to be significantly lower for ring-type processes as compared to a simple exchange process between 2 sites [22].

The spectral holes were considerably more stable in the compounds with only cationic disorder. For example, in $Ca_{0.2}Sr_{0.8}FCl$ host (compound 'a' in Fig. 2) no hole decay was observed within 2 h even at 430 K (the highest temperature probed).

3. Conclusions

In conclusion we note that the title compound family provides a certain domain in the frequency scale where the high-temperature hole burning can be realized on Sm^{2+} f–f transition(s). This domain is ultimately given by the dotted curve in Fig. 2(A) ($^5D_1$–$^7F_0$ transition). Its low frequency side is principally limited by the increasing strength of the crystal field (which finally inverts the positions of the excited $^5D_{0,1}$ and lowest 5d levels), and the high frequency side by the decreasing Debye temperature. These main limits may be thought to be rather general, at least for the fluoride-based materials.

The general intrinsic reason for hole filling at the sequential burning in Sm-doped materials [1, 5] is the generation of 'attractive' Sm^{3+} traps in the hole burning process. Consequently, parallel burning of holes (or time-domain recording) is generally favorable in case of photoionization mechanisms with distributed electron traps. The most critical factors for the possible practical use of Sm-doped solids are the hole burning efficiency and the availability of electron traps. The last factor determines (together with the solubility) the Sm^{2+} maximum concentration and hence the geometry of the material required for an acceptable optical density.

Finally, it was demonstrated that the dynamics of the disordered hosts, where Sm^{2+} can be stabilized and where f–f transitions can be seen, may be probed by spectral hole burning at rather high temperatures.

This work was supported by the 'Optique' priority program of the Board of the Swiss Federal Institutes of Technology and by Swiss National Science Foundation.

References

[1] R. Jaaniso, H. Bill, Europhys. Lett. 16 (1991) 569.
[2] K. Holliday, C. Wei, M. Croci, U.P. Wild, J. Lumin. 53 (1992) 227.
[3] K. Hirao, S. Todoroki, N. Soga, J. Lumin. 55 (1993) 217.
[4] K. Hirao, S. Todoroki, D.H. Cho, N. Soga, Opt. Lett. 18 (1993) 1586.
[5] A. Kurita, T. Kushida, T. Izumitani, M. Matsukawa, Opt. Lett. 19 (1994) 314.
[6] W.E. Moerner, (ed.), Persistent Spectral Hole Burning: Science and Applications, Topics in Current Physics 44 (Springer, Berlin, Heidelberg, 1988).
[7] S.A. Hodorowicz, E. Hodorowicz, H.A. Eick, J. Solid State. Chem. 50 (1983) 180.
[8] H. Hagemann, F. Kubel, H. Bill, Mat. Res. Bull. 28 (1993) 353.
[9] R. Jaaniso, H. Hagemann, H. Bill, J. Chem. Phys. 101 (1994) 10323.
[10] L. Zhang, J. Yu, S. Huang, J. Lumin. 45 (1990) 301.
[11] J.D. Eshelby, Solid State Phys. 3 (1956) 79.
[12] B. Birang, A.S.M. Mahbub'ul Alam, B. Di Bartolo, J. Chem. Phys. 50 (1969) 2750.
[13] R. Jaaniso, H. Bill, J. Phys.: Condens. Matter 5 (1993) 5921.
[14] A. Winnacker, R.M. Shelby, R.M. Macfarlane, Opt. Lett. 10 (1985) 350.
[15] D.E. McCumber, M.D.Sturge, J. Appl. Phys. 34 (1963) 1682.
[16] R. Jaaniso, H. Hagemann, F. Kubel, H. Bill, Chimia 46 (1992) 133.
[17] Y. Dossmann, R. Kuentzler, M. Sieskind, D. Ayachour, Solid State Commun. 72 (1989) 377.
[18] M. Fischer, M. Sieskind, A. Polian, A. Lahmar, J. Phys.: Condens. Matter 5 (1993) 2749.
[19] R. Jaaniso, M. Schnieper, D. Lovy, H. Bill, to be published.
[20] J. Zhang, S. Huang, J. Yu, Opt. Lett. 17 (1992) 1146.
[21] R.J. Borg, G.J. Dienes, An Introduction to Solid State Diffusion (Academic Press, Boston, 1988).
[22] C. Zener, Acta Cryst. 3 (1950) 346.